HHS Public Access

Author manuscript

J Neurosurg. Author manuscript; available in PMC 2020 November 17.

Published in final edited form as:

J Neurosurg. ; : 1–10. doi:10.3171/2019.2.JNS19271.

Degeneration of the lateral geniculate nuclei from pituitary adenoma compression detected by 7T ultra-high field MRI predicts vision recovery following surgical decompression of the optic chiasm

John W. Rutland, B.A.[1,2], **Javin Schefflein, M.D.**[3], **Annie Arrighi-Allisan, B.A.**[2], **Daniel Ranti, B.S.**[2], **Travis Ladner, M.D.**[2], **Akila Pai, B.S.**[2], **Joshua Loewenstern, B.A.**[2], **Hung-Mo Lin, PhD**[4], **James Chelnis, M.D.**[5], **Bradley N. Delman, M.D., M.S.**[3], **Raj K. Shrivastava, M.D.**[2], **Priti Balchandani, PhD**[1]

[1]Translational and Molecular Imaging Institute, Icahn School of Medicine at Mount Sinai, New York, New York, United States

[2]Department of Neurosurgery, Icahn School of Medicine at Mount Sinai, New York, New York, United States

[3]Department of Radiology, Icahn School of Medicine at Mount Sinai, New York, New York, United States

[4]Department of Population Health Science and Policy, Mount Sinai Hospital, New York, New York, United States

[5]Department of Ophthalmology, Icahn School of Medicine at Mount Sinai, New York, New York, United States

Abstract

Object—Predicting vision recovery following surgical decompression of the optic chiasm in pituitary adenoma patients remains a clinical challenge, as there isdue to significant variability in postoperative visual function that remains unreliably explained by current prognostic factors. Available literature inadequately characterizes alterations in adenoma patients involving the the lateral geniculate nucleus (LGN). This study examined LGN degeneration association with chiasmatic compression as well as retinal nerve fiber layer (RNFL), pattern standard deviation (PSD), mean deviation (MD), and postoperative vision recovery. PSD is PSD is the degree of difference between the measured visual field pattern, and MD is the average of the difference from the age-adjusted normal value.

Methods—A prospective study of 27 pituitary adenoma patients and 27 matched healthy controls was conducted. Participants were scanned on a 7 Tesla scanner, and three independent readers measured the LGN at its maximum cross-sectional area on coronal T1-weighted MPRAGE

Corresponding Author: John Rutland, Translational and Molecular Imaging Institute, Icahn School of Medicine at Mount Sinai, 1470 Madison Avenue; Floor 1, New York, NY 10029, jack.rutland@icahn.mssm.edu, Tel: 973-255-6562.

7.Competing interests

The authors report no competing interests.

imaging. Readers were blinded to diagnosis and to each other's measurements. Neuro-ophthalmology, including RNFL, MD, and PSD, was acquired for 12 patients, and postoperative visual function was collected on patients who underwent surgical chiasmal decompression. LGN areas were compared using two-tailed t-tests.

Results—The average LGN cross-sectional area of adenoma patients was significantly smaller than that of controls (13.8 mm^2 vs. 19.2 mm^2, $P<0.0001$). Average LGN cross-sectional area correlated with mean deviation (r = 0.67, $P=0.04$), PSD (r=−0.62, $P=0.02$) and retinal nerve fiber layer thickness (r = 0.75, $P=0.02$). LGN cross-sectional area in adenoma patients with chiasm compression was 26.6% smaller than in patients without compression ($P=0.009$). The average tumor volume was 7902.7 mm^3. Patients with preoperative vision impairment showed 29.4% smaller LGN cross-sectional areas than patients without deficits ($P=0.003$). Patients who experienced improved postoperative vision had LGN cross-sectional areas that were 40.8% larger than patients without postoperative improvement ($P=0.007$).

Conclusions—The authors demonstrate novel *in vivo* evidence of LGN volume loss in pituitary adenoma patients, and correlate imaging with neuro-ophthalmology and postoperative vision recovery. Morphometric changes to the LGN may reflect anterograde trans-synaptic degeneration. These findings indicate that LGN degeneration may be a marker of optic apparatus injury from chiasm compression, and may be useful in predicting vision recovery following adenoma resection.

Keywords

Chiasm compression; lateral geniculate nucleus; MRI; pituitary adenoma; trans-synaptic degeneration; neurosurgery

1. Introduction

Pituitary adenomas are benign tumors that account for nearly 15% of all intracranial neoplasms [6], with estimated prevalence ranging from 14.4% by autopsy to 22.5% by imaging.[13] The pituitary gland resides within the sella turcica, centered approximately 1 cm inferior to the optic chiasm. While many pituitary adenomas may be clinically occult, suprasellar extension and subsequent compression of the anterior optic apparatus leads to visual field defects (VFDs) in as many as 75% of patients.[33] Microadenomas (dimension<1 cm) rarely cause vision impairment as they are accommodated within the space between the dorsum sella and chiasm, while macroadenomas (dimension>1 cm) are more likely to cause mass effect on the chiasm and resultant VFDs. VFDs classically manifest as bitemporal hemianopia, reduced visual acuity, and diplopia.[1] Impairment of ocular movement may accompany vision loss if other cranial nerves become compressed.

Surgical resection is effective in halting and reversing vision loss by pituitary adenoma. Endoscopic endonasal surgery has proven to be particularly efficacious in decompressing the chiasm and alleviating VFDs, perhaps due to shorter operation duration and reduced need for skeletal disassembly and brain retraction compared with traditional open approaches.[33] However, suboptimal visual outcomes following resection are not uncommon. Absence of visual improvement has been reported in 26–80% of patients following surgery[7, 11], and

postoperative worsening vision has been reported in approximately 5%.[27] Various factors have been shown to be associated with postoperative vision recovery, including degree of chiasm compression, tumor volume, thickness of retinal nerve fiber layer (RNFL), and duration of vision impairment.[27] However, factors that differentiate patients who recover vision from those who either do not recover or continue to lose vision are not adequately described. Furthermore, there are conflicting reports of recovery predictors in the literature, [7,34,37] therefore, identification of novel markers of postoperative vision recovery is clinically valuable.

The lateral geniculate nucleus (LGN) is the major relay point for vision in the thalamus. It receives axonal input from the optic tracts and sends its own projections to the primary visual cortex (V1) via the optic radiations. Historically, boundaries of thalamic sub-regions have been difficult to delineate *in vivo* at clinical field strengths due to the subtle signal differences between the individual nuclei. However, ultra-high field MRI scanners, such as those operating at 7 Tesla (7T), have increased both spatial resolution and tissue signal, allowing visualization of anatomy that is undetectable at lower field strengths. With the high signal-to-noise ratio and submillimeter resolution afforded by 7T MRI, the LGN can be reproducibly identified and measured on T1-weighted sequences *in vivo*. Recent studies have reported volume reduction in the LGN of patients with disease of the anterior visual pathway, including glaucoma[9,17,18,27] and optic neuritis.[12] These are thought to reflect atrophic changes caused by trans-synaptic degeneration. While structural alterations to the posterior visual pathway have been reported in patients with chiasmatic compression by pituitary adenomas,[30,36,39] morphometric changes to the LGN have not yet been elucidated.

The purpose of the current study is to employ ultra-high field MRI to measure the LGN and determine whether i) degeneration is present in pituitary adenoma patients, ii) LGN atrophy correlates with neuro-ophthalmologic findings, and iii) morphometric alterations to the LGN predict vision recovery following decompression surgery.

2. Materials and methods

2.1 Participants

Approval was obtained from the local Institutional Review Board before recruitment. 27 patients [13 females, mean age 41.3 years, standard deviation (SD) 14.7 years; 14 males, mean 49.5 years, SD 11.3 years] with pituitary adenomas that were scheduled for resective surgery were recruited through their neurosurgeon (RS) at the Mount Sinai Medical Center between September 2014 and August 2018. Patients were age- and gender-matched with 27 neurologically and psychiatrically healthy controls [13 females, mean age 40.4 years, SD 11.9 years; 14 males, mean 47.7 years, SD 7.5 years]. All participants provided written informed consent prior to the study.

2.2. Imaging protocol

Participants were scanned under our Institutional Review Board-approved protocol using a 7T whole body scanner (Magnetom, Siemens Healthcare, Erlangen, Germany). A SC72CD gradient coil was used (G_{max}=70 mT/m, max slew rate = 200T/m/s), with a single channel

transmit and 32-channel receive head coil (Nova Medical, Wilmington, MA, USA). The scanning protocol included a coronal oblique T_1-weighted MPRAGE sequence with the following parameters: TE (ms)=1.95, TR(ms)=3000, flip angle (FA)=7°, field of view(FOV)=520×640-mm^2, slices=224, resolution=0.7-mm^3 isotropic.

2.3 Chiasm morphometry

An expert neuroradiologist (BD) measured the net center deflections of the optic chiasm. The reference line of the chiasm was established by connecting the lateral-most aspects of the mid-chiasm as visualized in the coronal plane. Perpendicular calipers were projected from the reference line to the superior and inferior margins of the chiasm at the point of maximal deflection. The average of these values represents the greatest deviation of the central chiasm, and differences between these two values corresponds with chiasm thickness at maximal deflection. Examples of normal and compressed optic chiasms are shown in Figure 1.

2.4 LGN measurements

Image analysis was performed by three independent readers that were blinded to each other's results. Only slices that were posterior to the pituitary gland were available during LGN measurement, so that readers were blinded to gross pituitary size as well. Image analysis was performed using Osirix version 9.0.2 (Pixmeo, Geneva, Switzerland). LGNs were identified on coronal T1-weighted MPRAGE images by their dark signal intensity surrounded by higher signal intensity white matter tracts. Boundary landmarks used to identify the LGN included the ambient cistern, medial geniculate nucleus, and optic radiations. The three readers independently identified slices where LGN showed the greatest cross-sectional area. Measurements from the three readers were averaged to quantify association with visual degeneration and recovery, and values were also correlated for inter-observer characterization.

2.5 Neuro-ophthalmological evaluation

12 of the patients in this study underwent neuro-ophthalmological examination prior to surgery. Neuro-ophthalmologic examination consisted of visual field by Humphrey Visual Field Analyzer and optical coherence tomography (OCT) by Zeiss Cirrus HD-OCT or Heidelberg Spectralis SD-OCT. OCT was used to survey retinal nerve fiber layer (RNFL) in micrometers and Humphrey perimetry 30–2 or 24–2 visual field testing was used to determine the presence of visual field defects and calculate the mean deviation (MD) and pattern standard deviation (PSD). The reliability criteria used were fixation losses less than 30%, as well as false positive and false negative errors less than 30%. Ocular examination included slit-lamp and dilated fundus examination. To determine postoperative vision recovery, a subjective designation of vision improvement, no change, and visual decline was made by the operating neurosurgeon during the weeks following the surgery.

2.6 Statistical analysis

Statistical analysis was performed using SAS v9.4 (SAS Institute Inc, Cary, NC). Intra-class coefficient (ICC) was used to determine agreement between raters. Mixed effects model for

repeated measures was used to estimate the least squares means for LGN cross-sectional area. Subsequent contrasts among raters and between groups were based on the least squares means. The model included fixed effects (rater, group and rater by group interaction) and assumed an unstructured variance-covariance structure of the repeated measures (by different raters). For calculation of the overall intraclass coefficient (ICC), the model only considered patients as random effect. Wilcoxon-rank two-tailed t-tests were used to determine group differences. Pearson's correlation coefficients were calculated to evaluate associations between LGN areas and neuro-ophthalmological results. LGN cross-sectional areas were averaged across left and right hemispheres because each LGN receives projections from both retinas. Averages of the three readers' measurements were used for correlation analysis.

3. Results

27 patients with pituitary adenomas (4 microadenomas, 23 macroadenomas) and 27 healthy controls underwent neuroimaging. Clinical features of patients are shown in Table 1. Within the adenoma group, 20 patients (74.0%) had chiasm compression diagnosed on preoperative imaging, and 17 (63.0%) patients had preoperative vision impairment. Preoperative neuro-ophthalmological examination was performed on 12 of the adenoma patients. 23 patients underwent endoscopic endonasal surgery with the goal of gross total resection. Among the 15 patients who experienced preoperative vision impairment who proceeded to surgery, 8 (53.3%) reported improved visual function following surgery, while 7 patients (46.7%) experienced no change in vision. No patients experienced visual decline following surgery.

3.1 Neuro-ophthalmology

Preoperative neuro-ophthalmological examination was acquired for 12 out of the 27 patients. Humphrey Visual Field Analyzer was performed with 12 patients and OCT was acquired for 9 patients. An example of OCT and Humphrey Visual Field Analyzer outcomes is shown in Figure 2. The average MD and PSD were −6.5 dB (σ=7.7 dB) and 4.8dB (σ=3.2 dB), respectively. The average RNFL thickness was 76.3 μm (σ=19.9 μm). Results of neuro-ophthalmological examination are shown in Table 1. MD was correlated with LGN cross-sectional area (r=0.67, P=0.04). PSD was negatively correlated with LGN cross-sectional area (r=−0.61, P=0.02). Lastly, RNFL thickness was positively correlated with LGN cross-sectional area (r=0.75, P=0.02). These results are shown in Figure 5. None of the patients with pituitary microadenoma exhibited preoperative visual impairment or received formal neuro-ophthalmological examination prior to surgery.

3.2 Cross-sectional area of LGN

A total of 108 LGN (54 in patients, 54 in controls) were identified and measured at their largest cross-sectional area (Figure 3). ICCs were 0.72 and 0.62 for the left and right LGN, respectively, yielding an overall ICC of 0.67. Results from the independent raters are shown in Figure 4. The average LGN cross-sectional areas in adenoma patients and controls were 13.8 mm^2 (σ=3.9 mm^2), and 19.2 mm^2 (σ=4.8 mm^2), respectively. The average LGN cross-sectional area for the subset of patients with microadenomas was 17.3 mm^2 (σ=1.3 mm^2). The ranges in LGN cross-sectional areas for adenoma patients, adenoma patients with

preoperative visual field defects, and controls were 7.55 mm^2-18.8 mm^2, 7.55 mm^2 –16.3 mm^2, and11.1 mm^2-25.8 mm^2 respectively. Reduction in LGN area in patients was significant ($P < 0.0001$). These results are summarized in Figure 4. Patients with chiasm compression had reduced LGN cross-sectional area compared with patients without chiasm involvement (μ=12.6 mm^2 and 17.2 mm^2, respectively, P=0.009). There was no significant difference in LGN cross-sectional area between controls (19.2 mm^2) and adenoma patients without chiasmal compression (17.2 mm^2, P=0.84). Patients with preoperative vision impairment also showed reduced LGN cross-sectional area (μ=11.8 mm^2) compared with patients without vision impairments (μ=16.7 mm^2, P=0.003). Lastly, patients who experienced vision improvement after surgery showed greater LGN cross-sectional area (μ=14.1 mm^2) than did patients without postoperative improvement (μ=8.3 mm^2, P=0.007). These results are shown in Figure 4.

3.3 Optic chiasm morphometry

The optic chiasm was identified in every participant in this study. The chiasmatic deflection was significantly greater in adenoma patients (μ=3.3 mm) than in controls (μ=0.3 mm, P<0.0001) (Figure 6). The thickness of the optic chiasm was significantly reduced in adenoma patients (1.7 mm) compared with controls (2.3 mm, P<0.0001). The average chiasm deflection and thickness for patients with microadenomas were 0.43 mm and 2.1 mm, respectively. There was a significant negative correlation between chiasm deflection and LGN cross-sectional area (r=0.52, P<0.0001). Chiasm thickness was positively correlated with LGN cross-sectional area (r=0.54, P<0.0001). The average tumor volume was 7902.7 mm^3 (σ = 5235.2 mm^3).

4. Discussion

Vision impairment is an important factor when considering resection of pituitary adenomas. Despite the development of less invasive approaches to the anterior skull base, such as transsphenoidal endoscopic endonasal surgery, a substantial proportion of adenoma patients fail to recover vision following chiasm decompression. While various factors have been implicated in preoperative prognosis, predicting vision recovery remains a clinical challenge.[7,34,37] The present study exploits high-resolution structural imaging at 7T to explore LGN degeneration as a novel marker of visual function and recovery from pituitary adenoma.

4.1 Trans-synaptic degeneration of the LGN

Trans-synaptic degeneration is the process by which secondary cell body apoptosis occurs following damage to neurons with which they synapses.[4,5,10] In this model, progression of disease spreads to interconnected brain regions within a neuronal system instead of merely spreading to adjacent unrelated structures. The human visual apparatus, including the retina, optic nerves, optic chiasm, LGN, optic radiations, and V1, provides a discrete neural system to study trans-synaptic degeneration.

While the existence of trans-synaptic degeneration within the human cerebellar [4] and motor [8] pathways has been recognized for years, this process has only recently been elucidated in

the human visual pathway, in part due to technological advances such as OCT. Retrograde trans-synaptic degeneration (rTSD), the process by which neuronal damage spreads from the visual cortex to the retina, has been observed in the human visual system following damage to the occipital lobe. [20,24] Anterograde trans-synaptic degeneration (aTSD) is the progression of neurodegeneration from the anterior visual pathway to posterior structures. Evidence of aTSD in human glaucoma [17, 9] and optic neuritis [22] has been reported in the form of LGN atrophy. aTSD is increasingly recognized as an important determinant of vision impairment in pituitary macroadenomas, where mass effect from an enlarging tumor mechanically compresses the optic chiasm. Diffusion tensor imaging studies have revealed reduced microstructural integrity of the optic tracts and radiations, the degree of which correlates with vision impairment in adenoma patients. [30,36,39] Cortical thinning in V1 has also been reported in patients with chiasm compression by pituitary adenoma.[39] However, degeneration of the LGN by pituitary adenomas has not yet been studied as it has in other diseases such as glaucoma. To our knowledge, the only prior association of degeneration of the LGNs with pituitary adenoma was in a post-mortem report from 1951, in which Samuel Gartner identified atrophy of the lateral geniculate nuclei in a single patient with chiasm compression from pituitary tumor.[14] In the present study, adenoma patients exhibited a 28.1% reduction of cross-sectional area on average across the left and right LGN compared with healthy controls. We hypothesize that aTSD is the neurobiological mechanism underlying this finding. A diagrammatic rendering of this process as a result of chiasm compression by pituitary adenoma is shown in Figure 7.

4.2 LGN association with chiasm morphometry

Several groups have studied the effects of suprasellar tumor volume on visual function, commonly reported as a positive correlation between volume and extent of visual impairment.[21,28] Chiasm deflection and LGN cross-sectional area were inversely related, such that greater chiasmatic distortion was associated with lesser LGN cross-sectional areas. Presumably, larger deflection can be attributable to greater tumor volumes. However, the authors chose to correlate imaging with chiasm deflection because tumor extension may not be suprasellar, and large tumors with extension in another dimension may not affect the chiasm as much as smaller tumors with purely suprasellar growth trajectory. Chiasm thickness positively correlated with LGN cross-sectional area, indicating that LGN degeneration becomes more apparent increasing degrees of chiasmatic thinning due to attenuation from adenoma-derived mass effect. These findings contribute to the hypothesis that aTSD occurs in the LGN of adenoma patients, as the extent of chiasm compromise correlated with LGN atrophy.

4.3 LGN degeneration correlates with visual function

In the present study, LGN cross-sectional area was positively correlated with MD. MD is the average of the difference from the age-adjusted normal value at various examination points, and characterizes the overall visual field depression. As MD becomes more negative, the overall visual field worsens. Normal MD values range between 0 dB and −2 dB.[43] The current analysis found that greater LGN cross-sectional areas were associated with less negative MD values, and this association is also consistent with prior studies that have reported a negative correlation between MD values and pituitary tumor volumes.

PSD was inversely related to LGN cross-sectional area, such that increasing PSD values correspond to reduced LGN cross-sectional areas. PSD is the degree of difference between the measured visual field pattern and the normal pattern or “hill” of vision. Greater PSD indicates a progressively irregular visual field pattern, representing localized sensitivity loss.[43] Our results are consistent with prior work that has positively correlated tumor volume with PSD.[29]

Lastly, the authors report a positive correlation between LGN cross-sectional area and RNFL thickness. The RNFL is a region of the retina composed of axons of the retinal ganglion cells. Topographic changes of the RNFL signify changes in the integrity of the retinal ganglion axons of the optic nerve.[31,38] While RNFL thickness has been shown to positively correlate with LGN volume in patients with glaucoma, [40] our study is the first to report a similar effect as a result of chiasm compression by pituitary adenomas.

4.4 LGN degeneration predicts vision recovery following decompression

While the regenerative features of retinal ganglion cells of the visual pathway have been well studied, the capacity of the LGN to recover after damage is inadequately described in the literature. In fact, vision recovery following LGN injury is not well defined. Permanent blindness has been shown to result from bilateral LGN infarcts.[35] Other studies have described reversible vision loss by lesion to the LGN in pathologies such as microangiopathy and myelinolysis.[41] *Ex vivo* studies demonstrating the existence of plasticity in the adult LGN support these accounts.[10,32] Recent reports from animal studies have shown remarkable restoration in LGN soma size that preceded vision recovery following retinal inactivation by neurotoxin.[10]

In the present study, LGN cross-sectional area significantly differed between patients who recovered vision after surgery (14.1 mm^2) and patients who exhibited no postoperative improvement (8.3 mm^2). This finding may hold prognostic value in patients with preoperative vision loss from pituitary adenomas. The authors hypothesize that this distinction may indicate a critical threshold of irreversible damage to LGN neurons, beyond which recovery is severely limited or impossible. Patients who experienced postoperative vision recovery had significantly less LGN volume loss before surgery. This may reflect preservation of enough parenchyma to permit plastic recovery of LGN neurons following decompression of the optic chiasm, resulting in gain of visual function. Patients with greater LGN atrophy showed no improvement after surgery, perhaps because damage to the LGN was too severe to allow plastic recovery after decompression. However, the data from the present study cannot indicate whether such a critical threshold exists and what cross-sectional area constitutes degeneration of the LGN. Future studies are required to quantitatively establish the cross-sectional area at which LGN degeneration is indicated as opposed to normal variance in structure size. This will help elucidate whether there is a critical threshold, below which recovery is unlikely, that can explicate the discrepancy in LGN degeneration between vision recovered and recalcitrant patients.

In addition to prognostic utility, our findings may also be useful in early detection of damage in the visual pathway and serve as an early indicator for neurosurgical intervention. Kristof et al. reported visual outcomes following pituitary adenoma resection and found that patients

with preoperative vision impairment recovered visual function, but not to the degree of patients without preoperative vision impairment.[26] Thus, surgery may be indicated in patients with chiasm involvement even before vision loss is reported, in order to prevent irreversible damage to the visual pathway. Imaging markers that are sensitive to early signs of visual pathway compromise, such as LGN degeneration, may be a valuable contributors to current prediction models of vision impairment.

4.5 Limitations and future directions

Because neuro-ophthalmological examination was not originally included in the protocol for this research study, this data was retrospectively analyzed and not all patients received formal examination. Out of the 27 patients in this study, only 12 received neuro-ophthalmological examination, of which 9 received OCT. Patients that did not experience preoperative visual impairment were not referred for examination and thus their neuro-ophthalmology data was not available for the present study. This smaller sample may have limited detectability of some correlations in this study. Additionally, postoperative neuro-ophthalmology was not available in the current study, and determination of postoperative visual function was made by a subjective designation of improvement, no change, and decline by the operating neurosurgeon. Follow-up neuro-ophthalmological examination will be a critical component of precisely quantifying postoperative vision recovery instead of using a coarse stratification method employed in the present study. Future work will involve obtaining detailed neuro-ophthalmological measures after surgery to elucidate the correlation between LGN degeneration and postoperative visual function.

Postoperative imaging is also an important component of future studies in this field. While 7T MRI permits greater contrast and higher resolution over clinical field strengths, the inclusion criteria for 7T imaging are more stringent than at lower field strengths. Metallic implants are often a contraindication for 7T MRI, making postoperative scanning logistically challenging. Transsphenoidal endoscopic endonasal procedures often do not involve the use of metallic implants and therefore are good candidates for such a longitudinal study. Postoperative imaging of the LGN is valuable in identifying structural substrates underlying vision recovery following surgery and characterizing plasticity features of the LGN that may confer vision recovery.

Numerous attempts have been made to segment the thalamus using an automated approach. Most of these methods have employed diffusion-weighted imaging to parcellate the thalamus based on local microstructure and connectomic properties.[3,25,44] Other groups have attempted to discern the thalamic nuclei based on functional connectivity.[19,23,25] These methods have shown varying degrees of accuracy in their ability to delineate nuclei boundaries, and multi-modal imaging methods appear to provide greater contrast between nuclei than conventional structural imaging. There have also been efforts to optimize structural T1-weighted sequences, enhancing the contrast between thalamic sub-regions and improving surgical targeting for techniques such as deep brain stimulation.[16,42] These methods have employed gray matter acquisitions with nulled white matter, and have demonstrated excellent contrast among the thalamic nuclei; however, they are still not commonly employed in clinical or research settings. Previous attempts to capture structural

LGN changes on T1-weighted imaging have typically relied on height [15] and cross-sectional area.[2] While some groups have reported LGN volumes, these acquisition methods have required proton density imaging [15,29], which was not included in the present study's imaging protocol. While volumetric analysis of the LGN in the context of chiasmal compression is an important line of enquiry accurate delineations of the structure could not be precisely visualized in this study. However, the cross-sectional areas of the LGN were precisely and reproducibly quantified in this study which the authors believe gave a very sensitive indicator of total LGN atrophy as indicated by the functional correlates with neuro-ophthalmology. The LGN profile was most conspicuous in the coronal plane and this delineation method was chosen to match techniques of prior investigations. Optimization of pulse sequences and development of robust reproducible segmentation methods, as well as widespread adoption of these tools into clinical workflow, will be critical for implementation of LGN degeneration as a predictor of vision recovery following pituitary adenoma resection and volumetric analysis. Optimized structural acquisitions, as well as automated thalamic segmentation methods, are currently being developed by our group.

Lastly, recent work has linked downregulation of the Akt signaling pathway in the LGN and V1 to aTSD following optic nerve transection in animal models.[45] Akt is an important signaling molecule responsible for neuronal survival and normal cell function. There is increasing evidence that Akt phosphorylation pattern plays a neuroprotective role in higher visual processing centers, such as LGN and V1. Identification of molecular signaling pathways that are dysregulated in aTSD may be valuable in identifying potential targets for novel therapeutic agents designed to reduce secondary neuronal damage in the visual pathway and preserve visual function in patients with pituitary adenoma or other pathology of the anterior visual pathway.

5. Conclusion

Vision impairment remains among the most debilitating comorbidities resulting from pituitary adenomas. Despite technological and procedural advances in the field of transsphenoidal endoscopic endonasal surgery and neuro-ophthalmology, postoperative vision recovery is variable and cannot be reliably predicted with current prognostic models. The present study demonstrates evidence of aTSD in the LGN among adenoma patients, and correlates structural alterations of the LGN with neuro-ophthalmology and vision recovery following surgery. aTSD in the LGN may account for the variability observed in postoperative vision recovery following tumor resection. While evidence of aTSD from pituitary adenoma has been established previously, it is believed that this is the first *in vivo* report of degeneration of the LGN. This structure appears to be vulnerable to secondary effects from chiasm compression, and ultra-high field MRI may offer valuable quantification of LGN degeneration to establish early indications for surgery and predict vision recovery following neurosurgical resection of pituitary adenomas.

Acknowledgments

We would like to thank Jill Gregory who provided medical illustration (Figure 7).

6. Funding

This work was funded by NIH R01 CA202911 and the Icahn School of Medicine Capital Campaign, Translational and Molecular Imaging Institute and Department of Radiology, Icahn School of Medicine at Mount Sinai.

Abbreviations:

aTSD	anterograde trans-synaptic degeneration
LGN	lateral geniculate nucleus
OCT	optical coherence tomography
RNFL	retinal nerve fiber layer
V1	primary visual cortex
VFD	visual field defect

References

1. Anderson JR, Antoun N, Burnet N, Chatterjee K, Edwards O, Pickard J, et al. Neurology of the pituitary gland. J Neurol Neurosurg Psychiatry 66:703–721, 1999 [PubMed: 10329742]
2. Anderson TJ, Halpern SD, Purves D. Correlated Size Variations in Human Visual Cortex, Lateral Geniculate Nucleus, and Optic Tract. J Neurosci 17:2859–2868, 1997 [PubMed: 9092607]
3. Behrens T, Johansen-Berg H, Woolrich M, Smith S, Wheeler-Kingshott C, Boulby P, et al. Non-invasive mapping of connections between human thalamus and cortex using diffusion imaging. Nat. Neurosci 6:750–757, 2003 [PubMed: 12808459]
4. Blackwood W. Transsynaptic Degeneration In: Blackwood W, Corsellis JAN, eds. Greenfield's Neuropathology. Third ed. Chicago: Year Book Med Pub, Inc:14–15, 1976
5. Bridge H, Jindahra P, Barbur J, Plant GT. Imaging reveals optic tract degeneration in hemianopia. Invest Ophthalmol Vis Sci 52:382–8, 2011 [PubMed: 20739474]
6. Chatzellis E, Alexandraki KI, Androulakis II, Kaltsas G. Aggressive pituitary tumors. Neuroendocrinology 101:87–104, 2015 [PubMed: 25571935]
7. Cohen AR, Cooper PR, Kupersmith MJ, Flamm ES, Ransohoff J. Visual recovery after transsphenoidal removal of pituitary adenomas. Neurosurgery 17:446–52, 1985 [PubMed: 4047355]
8. Cowan WM. Anterograde and Retrograde Trans-neuronal Degeneration in the Central and Peripheral Nervous System In: Nauta WJH, Ebbesson SOE, eds. Contemporary Research Methods in Neuro-anatomy. Heidelberg: Springer-Verlag, 217–51, 1970
9. Dai H, Mu KT, Qi JP, Wang CY, Zhu WZ, Xia LM, et al. Assessment of Lateral Geniculate Nucleus Atrophy with 3T MR Imaging and Correlation with Clinical Stage of Glaucoma. AJNR 32:1347–1353, 2011 [PubMed: 21757515]
10. Duffy KR, Fong MF, Mitchell DE, Bear MF. Recovery from the anatomical effects of long-term monocular deprivation in cat lateral geniculate nucleus. J Comp Neurol 526:310–323, 2018 [PubMed: 29023717]
11. Dutta P, Gyurmey T, Bansal R, Pathak A, Dhandapani S, Rai A, et al. Visual outcome in 2000 eyes following microscopic transsphenoidal surgery for pituitary adenomas: Protracted blindness should not be a deterrent. Neurol India 64:1247–1253, 2016 [PubMed: 27841194]
12. Evangelou N, Konz D, Esiri MM, Smith S, Palace J, Matthews PM. Size-selective neuronal changes in the anterior optic pathways suggest a differential susceptibility to injury in multiple sclerosis. Brain 124:1813–1820, 2001 [PubMed: 11522583]
13. Ezzat S, Asa SL, Couldwell WT, Barr CE, Dodge WE, Vance ML, et al. The Prevalence of Pituitary Adenomas: A Systematic Review. Cancer 101:613–9, 2004 [PubMed: 15274075]
14. Gartner S. Ocular pathology in the chiasmal syndrome. Am J Ophthalmol 34:593–6, 1951 [PubMed: 14819190]

15. Giraldo-Chica M1, Hegarty JP 2nd2, Schneider KA. Morphological differences in the lateral geniculate nucleus associated with dyslexia. NeuroImage: Clinical 7:830–836, 2015 [PubMed: 26082892]
16. Grewal SS, Middlebrooks EH, Kaufmann TJ, Stead M, Lundstrom BN, Worrell GA. Fast gray matter acquisition T1 inversion recovery MRI to delineate the mammillothalamic tract for preoperative direct targeting of the anterior nucleus of the thalamus for deep brain stimulation in epilepsy. Neurosurg Focus 45:E6, 2018
17. Gupta N, Greenberg G, de Tilly LN, Gray B, Polemidiotis M, Yücel YH. Atrophy of the lateral geniculate nucleus in human glaucoma detected by magnetic resonance imaging. Br J Ophthalmol 93:56–60, 2009 [PubMed: 18697810]
18. Gupta N, Ang LC, Noël de Tilly L, Bidaisee L, Yücel YH. Evidence for Neural Degeneration in Human Glaucoma Involving the Intracranial Optic Nerve, Lateral Geniculate Nucleus and Visual Cortex. Br J Ophthalmol 90:674–678, 2006 [PubMed: 16464969]
19. Hale JR, Mayhew SD, Mullinger KJ, Wilson RS, Arvanitis TN, Francis ST, et al. Comparison of functional thalamic segmentation from seed-based analysis and ICA. Neuroimage 114:448–465, 2015 [PubMed: 25896929]
20. Handley SE, Vasiliki PS, Liasis A. Trans-synaptic Retrograde Degeneration Following Hemispherectomy in Childhood. Neuroophthalmology 41:103–107, 2017 [PubMed: 28348634]
21. Ho RW, Huang HM, Ho JT. The Influence of Pituitary Adenoma Size on Vision and Visual Outcomes after Trans-Sphenoidal Adenectomy: A Report of 78 Cases. J Korean Neurosurg Soc 57:23–31, 2015 [PubMed: 25674340]
22. Jenkins TM, Ciccarelli O, Atzori M, Wheeler-Kingshott CA, Miller DH, Thompson AJ, et al. Early pericalcarine atrophy in acute optic neuritis is associated with conversion to multiple sclerosis. J Neurol Neurosurg Psychiatry 82:1017–21, 2011 [PubMed: 21297149]
23. Ji B, Li Z, Li K, Li L, Langley J, Shen H, et al. Dynamic thalamus parcellation from resting-state fMRI data. Hum Brain Mapp 37:954–967, 2016 [PubMed: 26706823]
24. Jindahra P, Petrie A, Plant GT: Retrograde trans-synaptic retinal ganglion cell loss identified by optical coherence tomography. Brain 132:628–34, 2009 [PubMed: 19224900]
25. Johansen-Berg H, Behrens TE, Sillery E, Ciccarelli O, Thompson AJ, Smith SM, et al. Functional–anatomical validation and individual variation of diffusion tractography-based segmentation of the human thalamus. Cerebr Cortex 15: 31–39, 2005
26. Kristof RA, Kirchhofer D, Handzel D, Neuloh G, Schramm J, Mueller CA, et al. Pre-existing chiasma syndromes do not entirely remit following transsphenoidal surgery for pituitary adenomas. Acta Neurochir 153:26–32, 2011 [PubMed: 20852901]
27. Laws ER Jr, Trautmann JC, Hollenhorst RW Jr. Transsphenoidal decompression of the optic nerve and chiasm: Visual results in 62 patients. J Neurosurg 46:717–722, 1977 [PubMed: 859014]
28. Lee JP, Park IW, Chung YS. The Volume of Tumor Mass and Visual Field Defect in Patients with Pituitary Macroadenoma. Korean J Ophthalmol 25:37–41, 2011 [PubMed: 21350693]
29. Lee JY, Jeong HJ, Lee JH, Kim YJ, Kim EY, Kim YY, et al. An Investigation of Lateral Geniculate Nucleus Volume in Patients With Primary Open-Angle Glaucoma Using 7 Tesla Magnetic Resonance Imaging. Invest Ophthalmol Vis Sci. 55:3468–76, 2014 [PubMed: 24722700]
30. Lilja Y, Gustafsson O, Ljungberg M, Starck G, Lindblom B, Skoglund T, et al. Visual pathway impairment by pituitary adenomas: quantitative diagnostics by diffusion tensor imaging. J Neurosurg 127:569–579, 2017 [PubMed: 27885957]
31. Loewenstern J, Hernandez CM, Chadwick C, Doshi A, Banik R, Sarkiss CA, et al. Optical coherence tomography in the management of skull base fibrous dysplasia with optic nerve involvement. World Neurosurg 109:e546–e553, 2018 [PubMed: 29038079]
32. Moore BD, Kiley CW, Sun C, Usrey WM. Rapid Plasticity of Visual Responses in the Adult Lateral Geniculate Nucleus. Neuron 71:812–9, 2011 [PubMed: 21903075]
33. Muskens IS, Najafabadi AH, Briceno V, Lamba N, Senders JT, van Furth WR, et al. Visual outcomes after endoscopic endonasal pituitary adenoma resection: a systematic review and meta-analysis. Pituitary 20:539–552, 2017 [PubMed: 28643208]

34. Müslüman AM, Cansever T, Yılmaz A, Kanat A, Oba E, Çavuşoğlu H. Surgical results of large and giant pituitary adenomas with special consideration of ophthalmologic outcomes. World Neurosurg 76:141–8, 2011 [PubMed: 21839965]
35. Moseman CP, Shelton S. Permanent blindness as a complication of pregnancy induced hypertension. Obstet Gynecol 100:943–5, 2002 [PubMed: 12423857]
36. Phal PM, Steward C, Nichols AD, Kokkinos C, Desmond PM, Danesh-Meyer H, et al. Assessment of Optic Pathway Structure and Function in Patients With Compression of the Optic Chiasm: A Correlation With Optical Coherence Tomography. Invest Ophthalmol Vis Sci 57:3884–3890, 2016 [PubMed: 27459665]
37. Powell M. Recovery of vision following transsphenoidal surgery for pituitary adenomas. Br J Neurosurg 9:367–373, 1995 [PubMed: 7546358]
38. Radius RL, de Bruin J. Anatomy of the retinal nerve fiber layer. Invest Ophthalmol Vis Sci 21:745–749, 1981 [PubMed: 7298277]
39. Rutland J, Padormo F, Yim C, Arrighi-Allisan A, Yao A, Lin HM, Chelnis J, Delman B, Shrivastava R, Balchandani P. Assessment of secondary white matter injury in the visual pathway by pituitary adenomas: A multimodal study at 7 Tesla MRI. J Neurosurg 18:1–10, 2019
40. Schmidt MA, Knott M, Heidemann R, Michelson G, Kober T, Dörfler A, et al. Investigation of lateral geniculate nucleus volume and diffusion tensor imaging in patients with normal tension glaucoma using 7 tesla magnetic resonance imaging. PLoS One 13:e0198830, 2018 [PubMed: 29879191]
41. Stem MS, Fahim A, Trobe JD, Parmar HA, Ibrahim M. Lateral geniculate lesions causing reversible blindness in a pre-eclamptic patient with a variant of posterior reversible encephalopathy syndrome. J Neuroophthalmol 34:372–6, 2014 [PubMed: 24739995]
42. Sudhyadhom A, Haq IU, Foote KD, Okun MS, Bova FJ. A high resolution and high contrast MRI for differentiation of subcortical structures for DBS targeting: the Fast Gray Matter Acquisition T1 Inversion Recovery (FGATIR). Neuroimage 47:T44–52, 2009 [PubMed: 19362595]
43. Tan N, Tham Y, Koh V, Nguyen D, Cheung C, Aung T, ey al. The Effect of Testing Reliability on Visual Field Sensitivity in Normal Eyes. Ophthalmology 125:15–21, 2018 [PubMed: 28863943]
44. Wiegell MR, Tuch DS, Larsson HB, Wedeen VJ. Automatic segmentation of thalamic nuclei from diffusion tensor magnetic resonance imaging. Neuroimage 19:391–401, 2003 [PubMed: 12814588]
45. You Y, Gupta VK, Graham SL, Klistorner A. Anterograde degeneration along the visual pathway after optic nerve injury. PLoS One 7:e52061, 2012 [PubMed: 23300590]

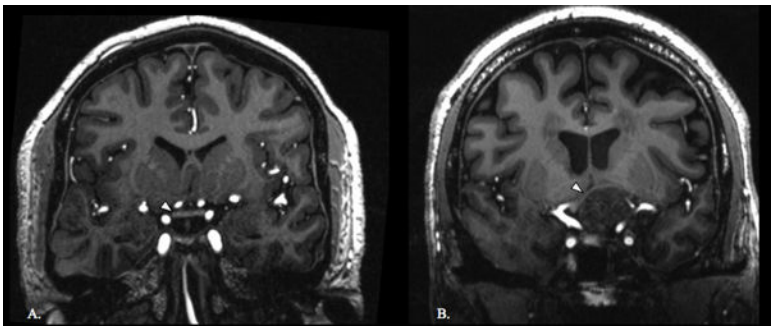

Figure 1.

Optic chiasm in control and adenoma patient. Coronal T1-weighted image of a normal optic chiasm (white arrowhead) in a control (A). Coronal T1-weighted image of an optic chiasm (white arrowhead) being compressed by a pituitary adenoma (B).

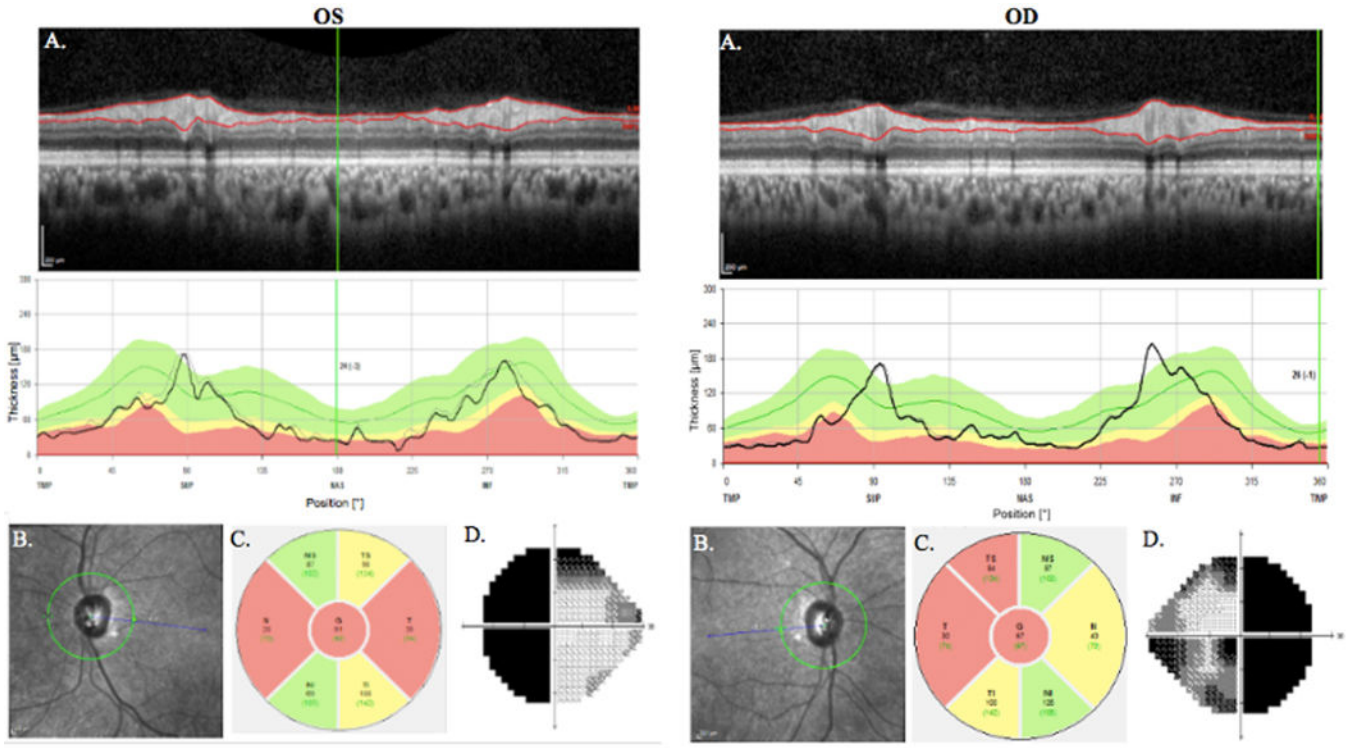

Figure 2.

Neuro-ophthalmology. These results are from the patient with pituitary adenoma in Figure 1. Results from optical coherence tomography showing reduced RNFL thickness in a patient with pituitary adenoma and significant chiasm compression (A). Regions of red are outside of normal limits. Grayscale plot of the optic nerve head as taken by OCT (B). Depiction of RNFL thickness with temporal field loss corresponding to nasal thinning. Areas out of normal limits are red and borderline areas are yellow (C). Gray plot results from Humphrey Visual Field Analyzer.

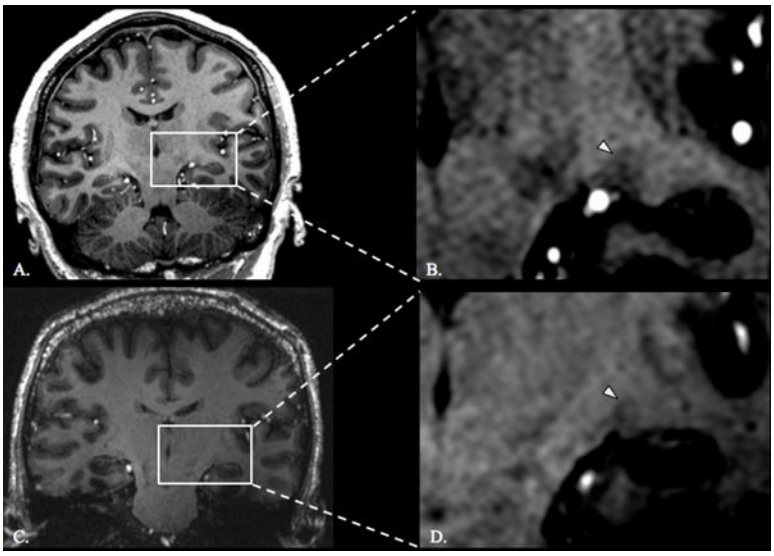

Figure 3.

LGN in control and adenoma patient. T1-weighted coronal slice through the LGN at the maximum cross sectional area of a healthy control (A) and a zoomed-in depiction of the left LGN (white arrowhead denotes the left LGN) (B). T1-weighted coronal slice through the LGN at the maximum cross sectional area of an adenoma patient with chiasm compression (C) and a zoomed-in depiction of the left LGN (white arrowhead denotes the left LGN) (D).

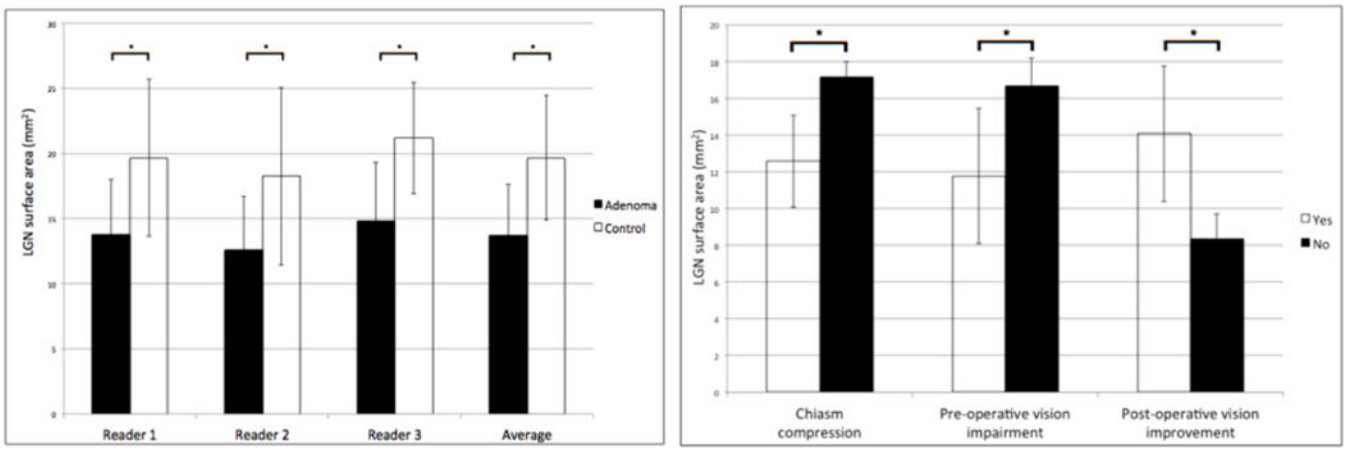

Figure 4.

Left: Bar graph showing the LGN cross-sectional area measurements acquired by 3 independent readers and the average LGN cross-sectional areas. *Right*: Bar graph showing LGN cross-sectional area as it related to disease features and response to surgery. Asterisk denotes significance, $P < 0.0001$.

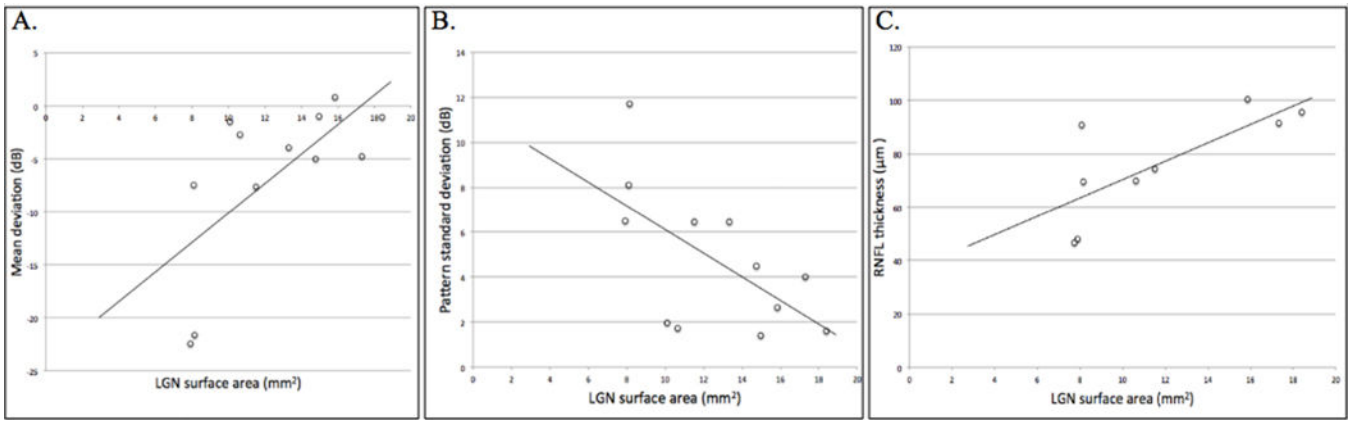

Figure 5.

Correlations between LGN cross-sectional area and mean deviation (r = 0.67, $P = 0.04$) (A), pattern standard deviation (r = −0.61, $P = 0.02$) (B), and RNFL thickness (r = 0.75, $P = 0.02$) (C) in adenoma patients.

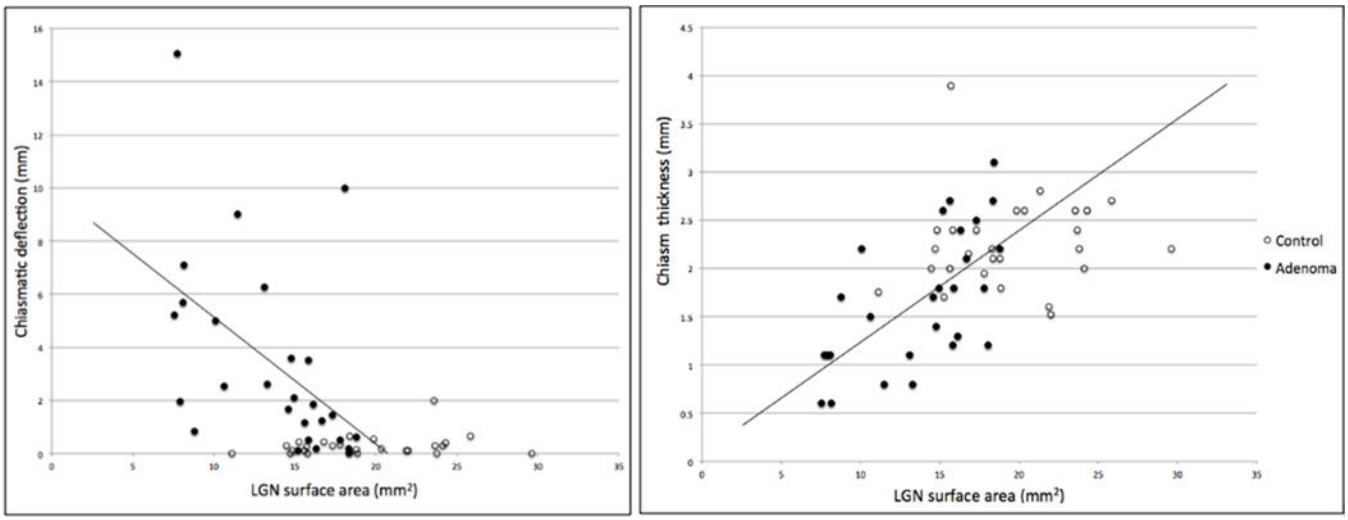

Figure 6.

Correlations between LGN cross-sectional area and optic chiasm morphometry in controls and adenoma patients. Correlation (r = −0.52, $P < 0.0001$) between LGN cross-sectional area and chiasmatic deflection (left). Correlation (r = 0.54, $P < 0.0001$) between LGN cross-sectional area and chiasm thickness.

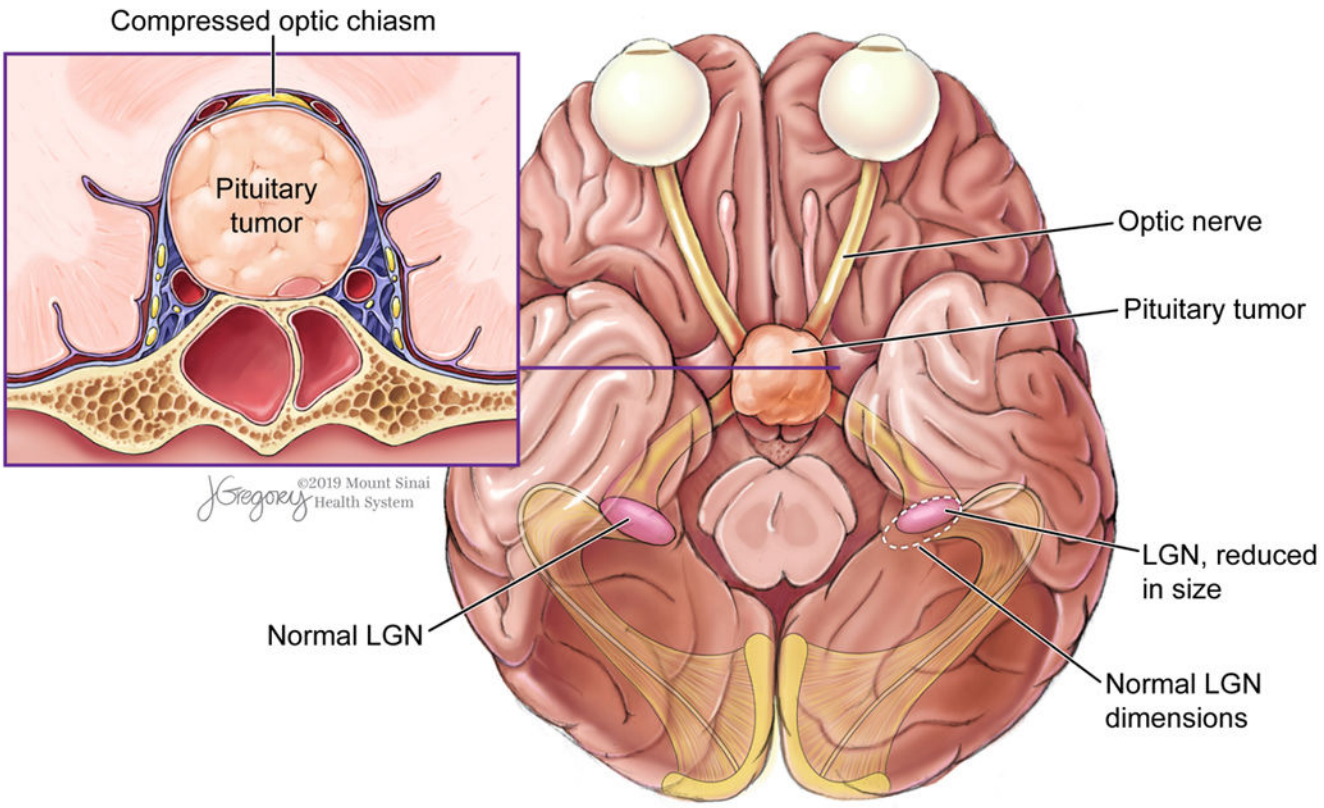

Figure 7.
Diagram of trans-synaptic degeneration of the LGN as a result of chiasmal compression by pituitary adenoma.

Table 1.

Disease features and surgical outcomes of 27 patients with pituitary adenoma.

Diagnosis	
Microadenoma, N (%)	4 (14.8)
Macroadenoma, N (%)	23 (85.2)
Imaging	
Chiasm compression, N (%)	20 (74.1)
Chiasm deflection, μ (SD)	3.3 (3.6)
Chiasm thickness (mm), μ (SD)	1.67 (0.7)
Preoperative visual function	
Impairment, N (%)	17 (63.0)
Neuro-ophthalmology, N (%)	12 (44.4)
MD (dB), μ (SD)	−6.5 (7.7)
PSD (dB), μ (SD)	4.8 (3.2)
RNFL (μm), μ (SD)	76.3 (19.9)
Proceeded to surgery, N (%)	23 (85.2)
Postoperative visual function	
Improvement, N (%)	8 (53.3)
No change, N (%)	7 (46.7)
Decline, N (%)	0 (0.0)